Supplementary Information (SI) for Physical Chemistry Chemical Physics.

Densification of Sodium and Magnesium Aluminosilicate Glasses at Ambient Temperature: Structural Investigations by Solid-state Nuclear Magnetic Resonance and Molecular Dynamics Simulations

Millena Logrado[1#], Yara Hellen Firmo Gomes,[2#] Tomiki Inoue[3], Shingo Nakane[3], Yoshinari Kato[3], Hiroki Yamazaki[3], Akihiro Yamada[4],

and Hellmut Eckert[2,5*]

[1] Eduard-Zintl-Institut für Anorganische und Physikalische Chemie, Technische Universität of Darmstadt, 64287 Darmstadt, Germany

[2] Instituto de Física de São Carlos, Universidade de São Paulo, Avenida Trabalhador São-carlense 400, São Carlos, SP 13566-590, Brazil

[3] Nippon Electric Glass Co., Ltd., 7-1, Seiran 2-chome, Otsu, Shiga 520-8639, Japan

[4] Department of Materials Chemistry, The University of Shiga Prefecture, 2500 Hassaka, Hikone, Shiga 522-8533, Japan

[5] Institut für Physikalische Chemie, Universität Münster, Corrensstraße 28-30, 48149 Münster, Germany

# equally contributing

* Corresponding author: email address: eckert@ifsc.usp.br;

SUPPORTING INFORMATION

I. Glass Preparation Details

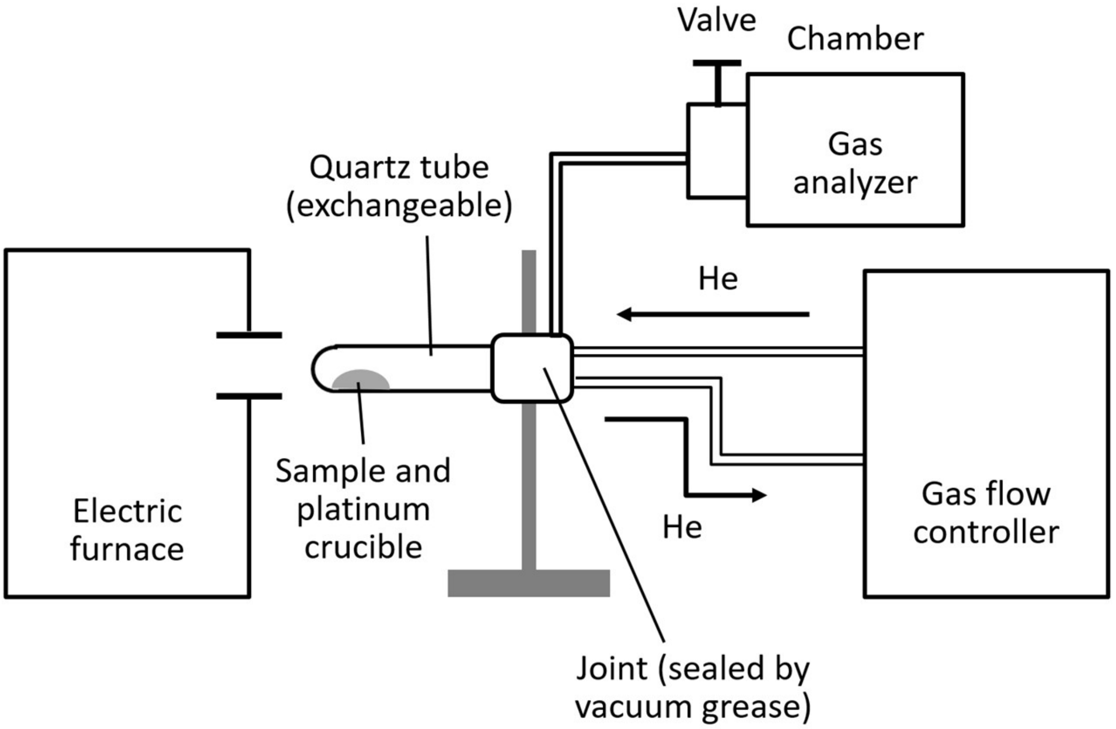

Figure S1: Experimental set-up for the preparation of the ^{17}O enriched glass samples.

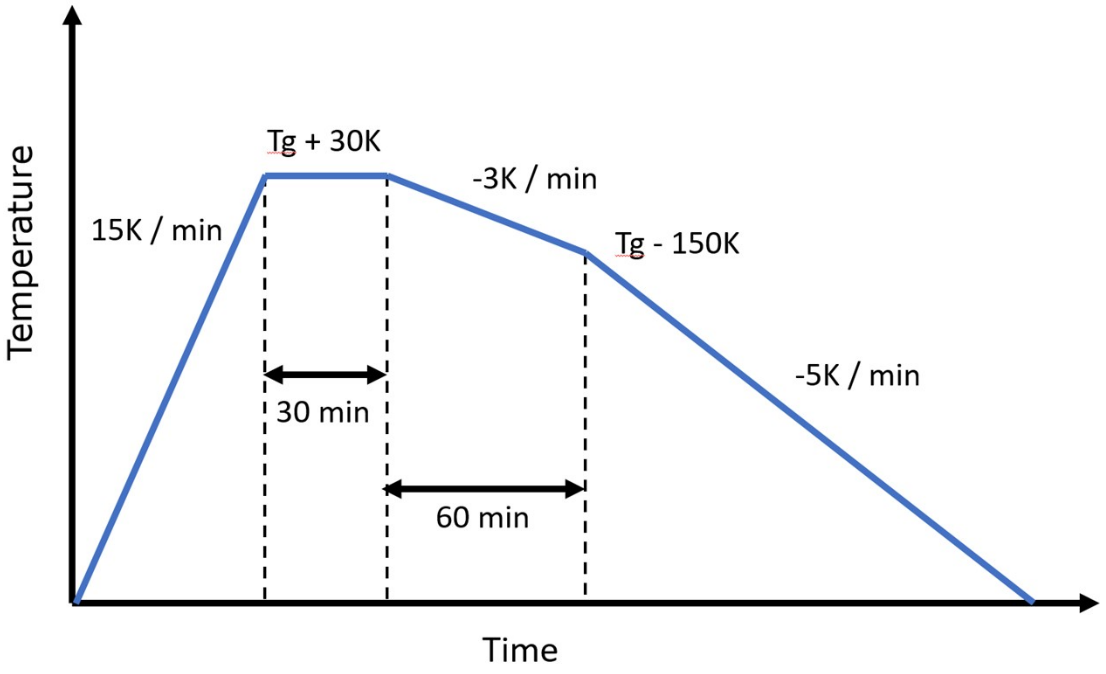

Figure S2: Annealing protocol for the glasses

II. Spectroscopic comparison of crushed vs. uncrushed samples

To address concerns about irreversible sample changes occurring upon crushing the samples for preparing powders for magic-angle spinning experiments, the samples prepared at 12 GPa were initially examined in the uncrushed state. This was possible both under static and slow MAS conditions on the compacted pieces within 7.5 mm rotors at 5.64 T for ^{29}Si, ^{27}Al, and ^{23}Na isotopes. The ^{29}Si-NMR results are shown in Figure S3, which compares the static Hahn Echo (red curve) and the rotor-synchronized Hahn Echo (HE) of the unground sample (blue curve) with synchronized HE performed on the ground samples. Lineshape parameters are listed in Table S1. Variations in the lineshape parameters (average isotropic chemical shifts and full width at half maximum) of the ground and the unground samples were within the typical error limits of ±1.0 ppm. Thus, within these given error limits the ^{29}Si MAS NMR experiments give no evidence of any significant effects due to sample crushing.

With the same color coding used for ^{29}Si, Figure S4 depicts the ^{27}Al-NMR data. In the Mg-containing samples, Al occurs in multiple coordination numbers, consistent with previously published results. The data obtained on the uncrushed sample measured at 5.64 T and the crushed sample measured at 14.1 T look very similar, although precise fitting was not possible as the limited spinning speed for the uncrushed sample was insufficient to eliminate spinning sidebands belonging to the central transition. For recording these spectra. ^{27}Al NMR pulse lengths were chosen to maximize signal intensities, and corresponded to flip angles larger than the recommended $\pi/12$ limit for strictly quantitative detection conditions. In the present case this was justified based on the nutation behavior of the three distinct Al coordination states and their similar nuclear electric quadrupolar coupling strengths (see Table S2).

Finally, Figure S5 shows the analogous results obtained for ^{23}Na NMR. Here the lineshape fit obtained at 5.64 T measured before sample grinding (HP) shows to be fully consistent with the results obtained on the ground samples measured at 14.1 T. Based on these preliminary studies the subsequent experiments were conducted on the crushed samples.

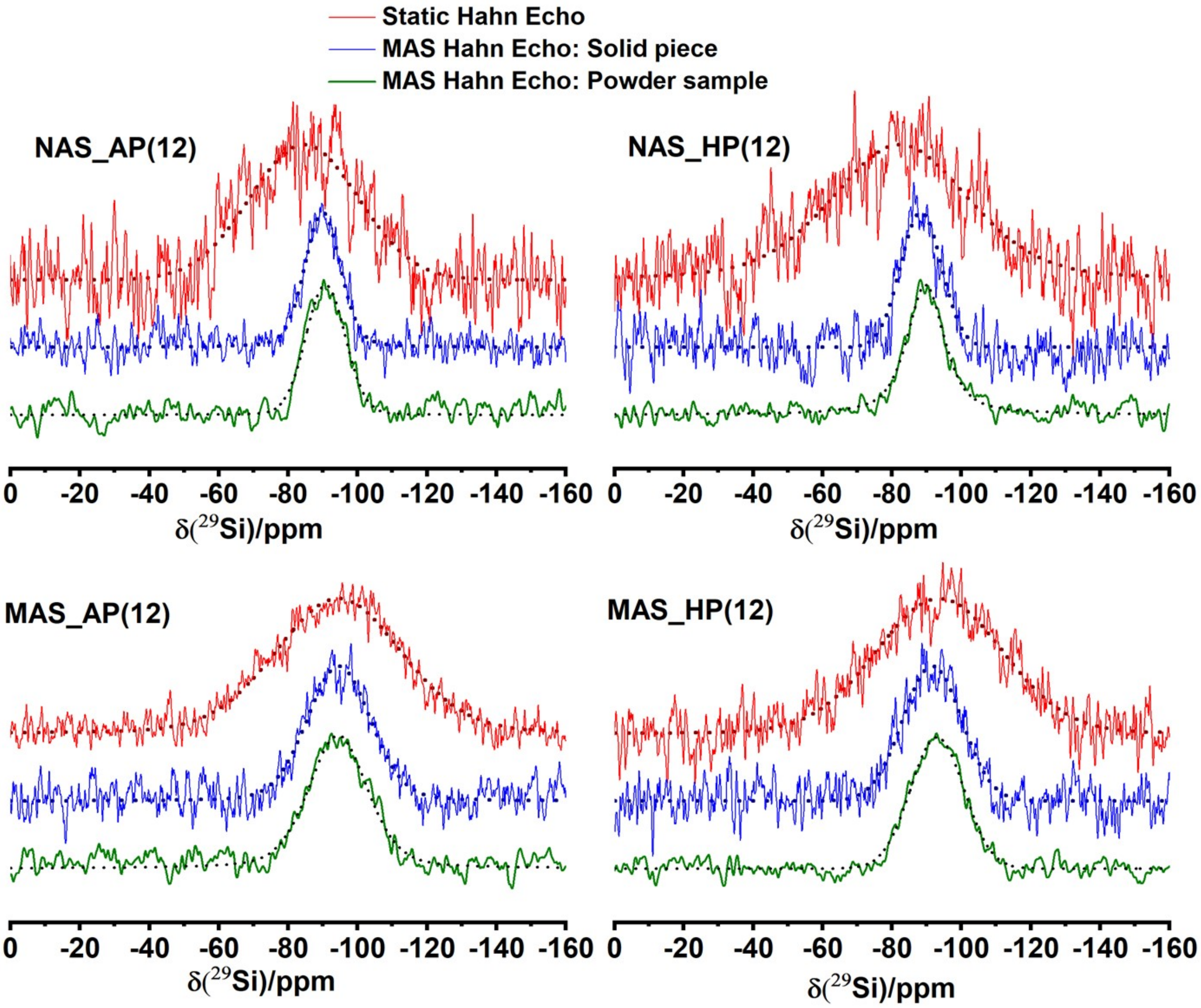

Figure S3: ^{29}Si static Hahn Echo (red) and MAS NMR spectra of solid glass pieces (blue) and of ground glasses (green) of samples NAS and MAS

Table S1: Average ^{29}Si MAS isotropic chemical shifts δ_{iso} and full widths at half maximum (*FWHM*) measured on the samples under study. Average isotropic chemical shifts were measured either by the first moment method or by an artificial two-component fit.

	Static HE		MAS HE - unground		MAS HE - ground	
	M_1\ Fit ±2/ppm	FWHM ±2/ppm	M_1\ Fit ±2/ppm	FWHM ±2/ppm	M_1\ Fit ±1/ppm	FWHM ±1/ppm
NAS-HP(12)	-80 \ -82	47	-90 \ -88	14	-91 \ -90	13
NAS-AP(12)	-85 \ -85	40	-90 \ -90	12	-91 \ -91	13
MAS-HP(12)	-93 \ -94	43	-92 \ -92	20	-93 \ -93	18
MAS-AP(12)	-95 \ -94	43	-95 \ -95	22	-95 \ -94	20

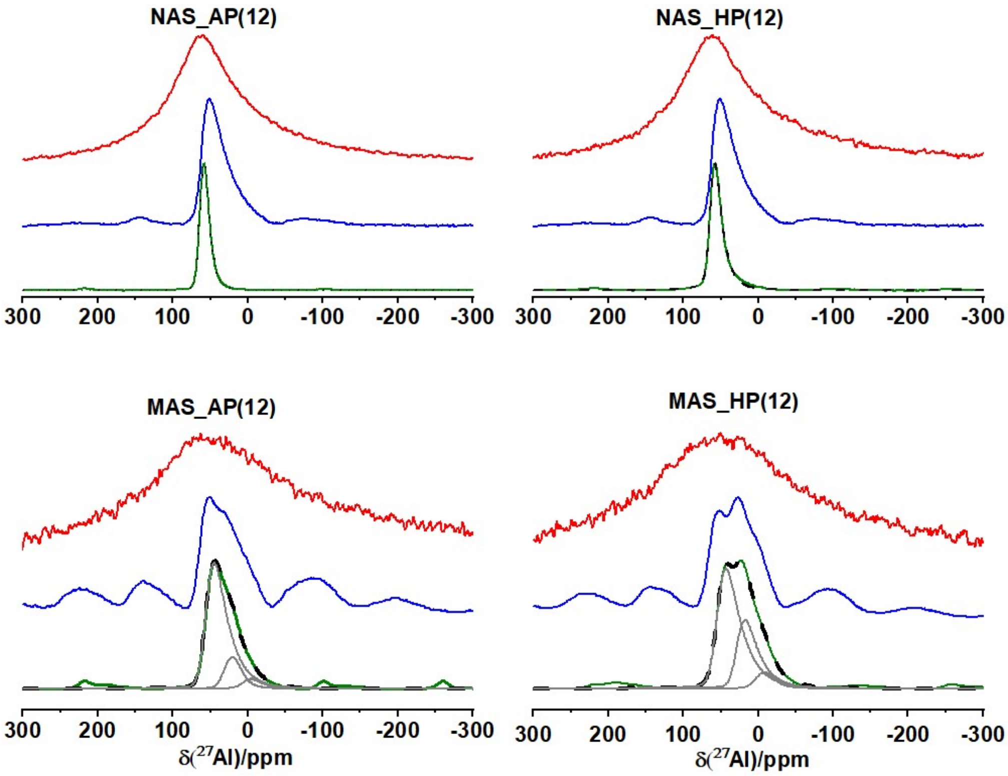

Figure S4: ^{27}Al static Hahn Echo (red) and MAS NMR spectra of solid glass pieces (blue) and of ground glasses (green) of samples NAS and MAS in HP(12) and AP conditions. Uncrushed samples were measured at 5.64 T and 6.5 kHz spinning frequency whereas crushed samples were measured at 14.1 T and 25 kHz spinning frequency. Gray curves indicate simulated signal components belonging to the different Al coordination states. Central transition resonances of spectra belonging to solid glass pieces are flanked by MAS sideband patterns.

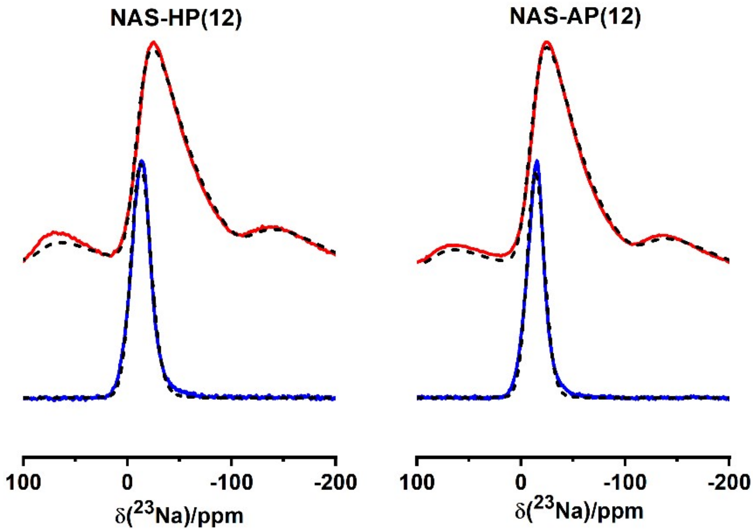

Figure S5: ^{23}Na MAS-NMR data on NAS-HP(12) (left) and NAS-AP(12) (right). The corresponding fits to a distribution of quadrupolar coupling constants, as implemented in the Czjzek model are shown as dashed curves. Red: unground sample, measured at 5.64 T with a rotor-synchronized Hahn spin echo method. Blue: ground sample, measured at 14.1 T using single-pulse NMR. The different appearances of the spectra of the ground and the unground samples are due to the difference in the magnetic field strengths

Table S2: ^{23}Na average isotropic chemical shifts $<\delta_{iso}^{cs}>$ and average magnitudes of nuclear electric quadrupolar coupling constants $<|C_q|>$, and full width at half maximum linewidth parameters *FWHM* of NAS glasses. The interaction parameters were deduced from single-site fits to the ^{23}Na MAS NMR lineshape using the Czjzek model implemented in the DMfit and ssNake simulation programs.

	Experimental condition	$<\delta_{iso}^{cs}>$ ppm	$<\|C_Q\|>$ MHz	*FWHM* ppm
NAS-HP(12)	5.7 T - unground[a]	-6 ± 2	2.9 ± 0.5	22 ± 2
	14.1 T - ground[b]	-8 ± 1	2.2 ± 0.2	19 ± 1
NAS-AP(12)	5.7 T- unground[a]	-7 ± 2	2.7 ± 0.5	22 ± 2
	14.1 T- ground[b]	-10 ± 1	1.8 ± 0.2	18 ± 1

[a] rotor-synchronized Hahn spin echo, [b]single-pulse acquisition

I. Supplemental Spectroscopic Characterization

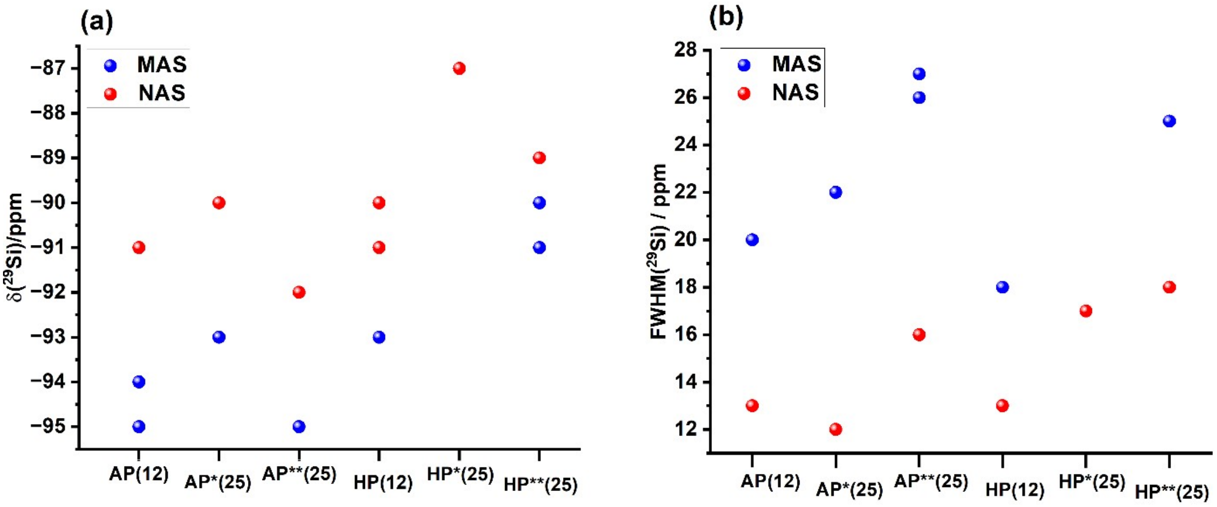

Figure S6: (a) Average ^{29}Si isotropic chemical shifts obtained either by First-Moment determination or spectral decomposition for the samples NAS and MAS in AP(12), AP*, AP**, HP(12), HP*(25), HP**(25) conditions. **(b)** Full width at half maximum (FWHM) obtained for spectral decomposition of same samples in the item (a).

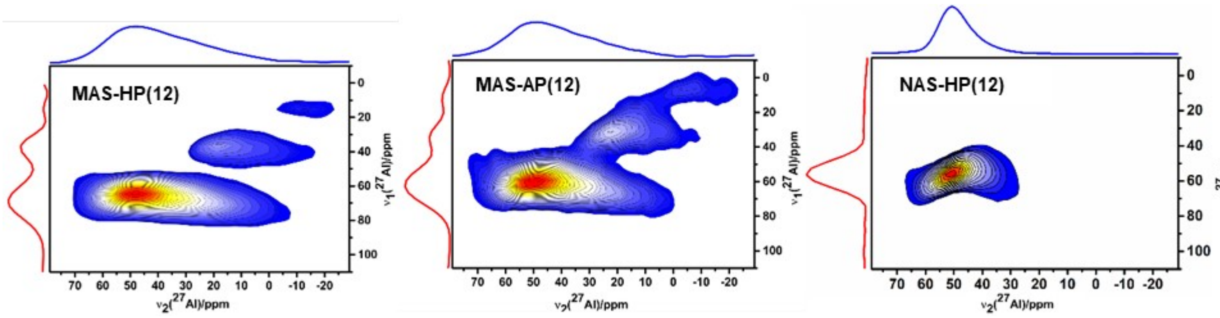

Figure S7: ^{27}Al TQMAS NMR spectra obtained, respectively, on the MAS-HP(12), MAS-AP(12) and NAS-HP(12) glasses of the present study measured at 14.1 T. The spectrum for NAS-HP(12) glass gives no evidence of higher-coordinated Al in the pressurized sample.

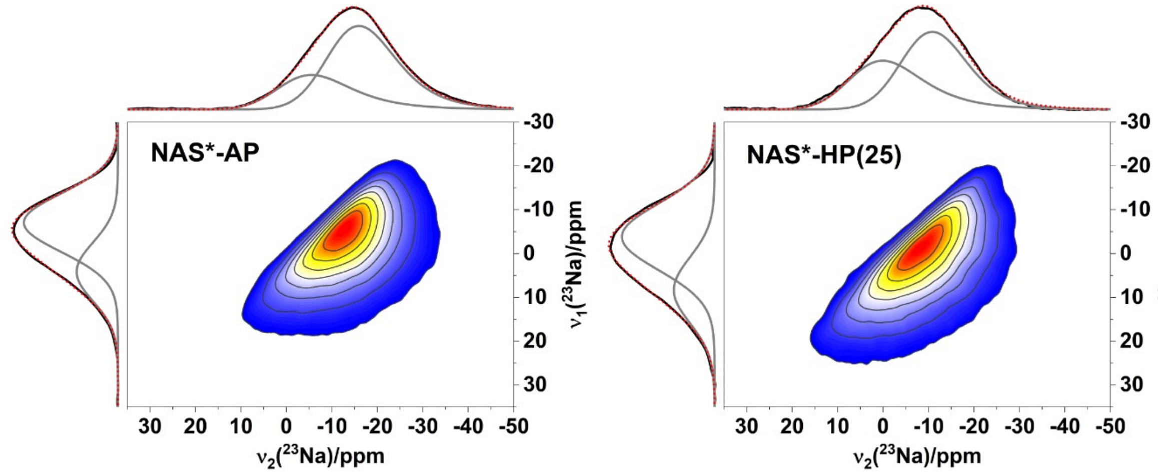

Figure S8: ^{23}Na TQMAS NMR spectra obtained, respectively, on the NAS*-AP and NAS*-HP(25) glasses of the present study measured at 14.1 T.

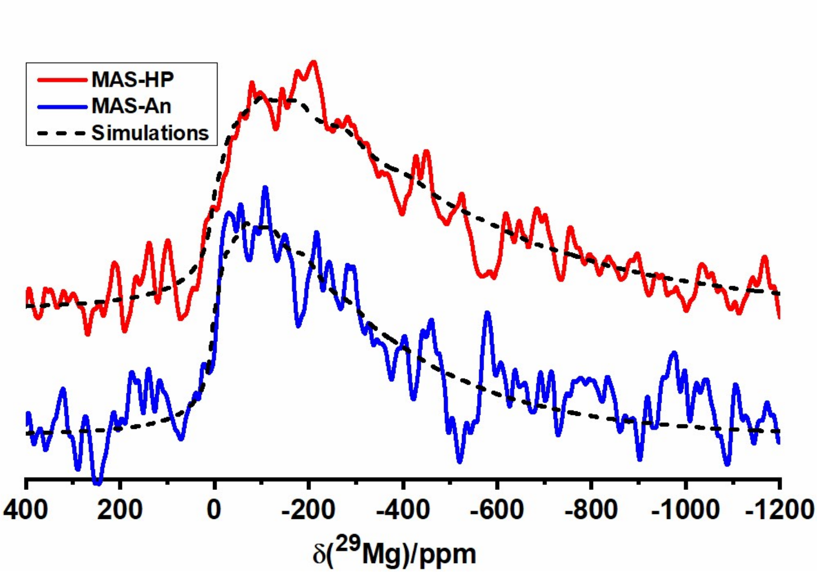

Figure S9: ^{25}Mg MAS NMR spectra of MAS-HP(12) and MAS-AP(12) glasses.

Table S3: ^{25}Mg MAS-NMR average isotropic chemical shifts $<\delta_{iso}^{cs}>$ and average magnitudes of nuclear electric quadrupolar coupling constants $<|C_q|>$, and full width at half maximum linewidth parameters FWHM of MAS glasses. These interaction parameters were deduced from fits to the ^{25}Mg MAS NMR lineshape measured at 14.1 T using the Czjzek model [53] implemented in the DMfit simulation program.

Sample	$<\delta_{iso}^{cs}>$ ±5/ppm	$<\|C_Q\|>$ ±2/MHz	*FWHM* ±5/ppm
MAS-HP(12)	7	8	18
MAS-AP(12)	14	7	10

Measurement comparison: NAS -AP and NAS**-HP(25)**

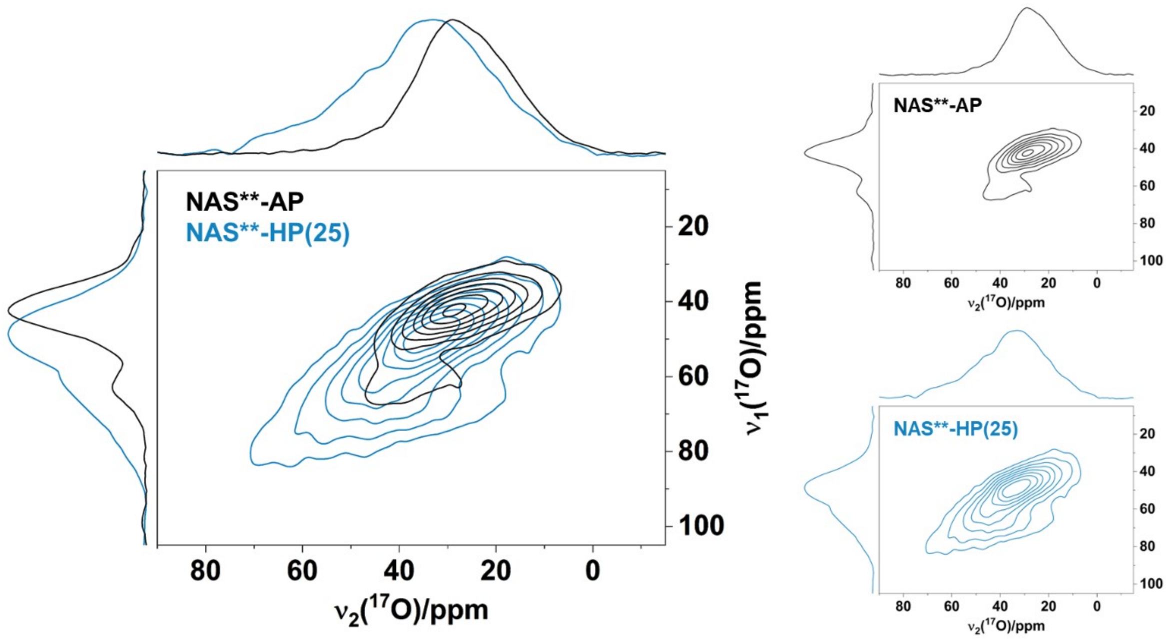

Measurement comparison – MAS-AP and MAS**-HP(25)**

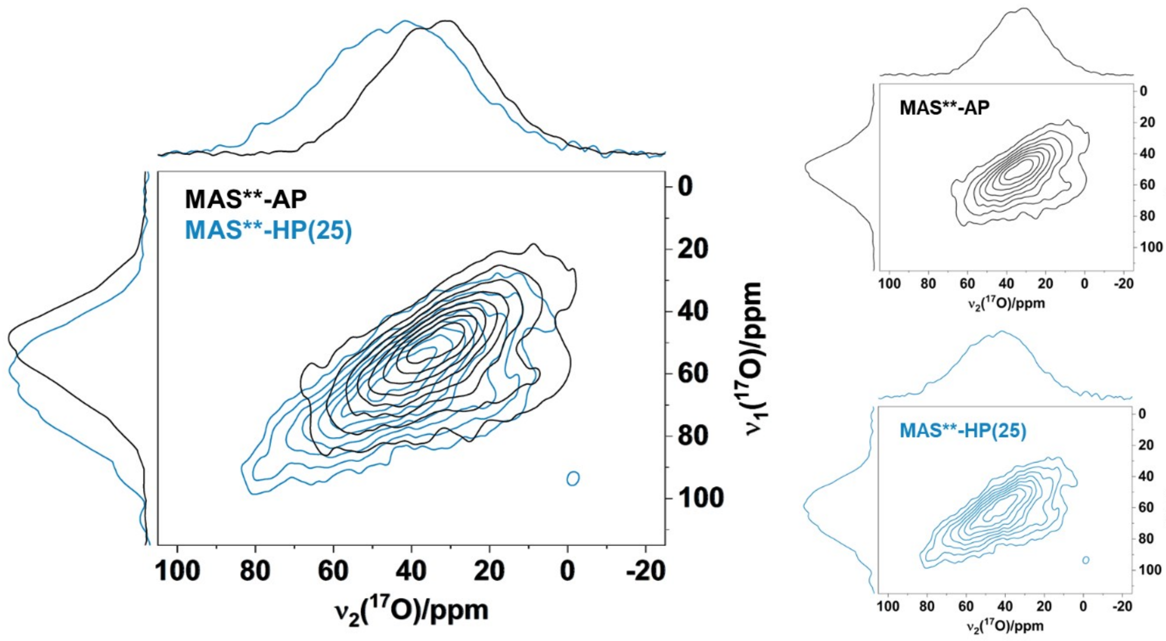

Figure S10: direct superposition of the ^{17}O TQMAS-NMR data of the NAS** and MAS** glasses in the AP and the HP(25) states.

Table S4: Numerical data of densification ratios as a function of pressure and parameters of the analytical approximation curves.

MD:

Pressure (P) / GPa	$\Delta\rho/\rho$ (%)		
	MAS	NAS	Silica
0	0	0	0
5	1.4	0.8	0.3
8	5.6	2.0	1.0
12	10.4	4.0	7.6
15	12.4	6.8	13.6
20	13.1	9.3	20.0
25	13.2	10.1	21.6

Experimental results:

MAS		NAS		Silica	
P / GPa	$\Delta\rho/\rho$(%)	P / GPa	$\Delta\rho/\rho$(%)	P / GPa	$\Delta\rho/\rho$(%)
0	0	0	0	0	0
2	0.2	2	0.1	8	0.5
3	0.1	6.6	2.1	12	4.1
6.1	1.4	7.1	1.7	20	20.0
7.1	4.9	12	3.4	25	21.0
7.2	3.2	25	6.0	-	-
12	7.5	-	-	-	-
25	9.0	-	-	-	-

Approximation curve :

$$f(x) = \alpha\left\{1 - \frac{1}{1 + \left(\frac{x}{\beta}\right)^{\gamma}}\right\}$$

Fitting parameters:

	α	β	γ
MAS-MD	13.55	8.73	3.97
NAS-MD	12.19	14.25	3.05
Silica-MD	22.63	13.77	5.25
MAS-Exp.	8.70	8.30	5.20
NAS-Exp.	7.07	12.30	2.45
Silica-Exp.	21.27	14.30	8.10